Iranian Journal of Medical Physics

ijmp.mums.ac.ir

Determination of Dose-Equivalent Response of A Typical Diamond Microdosimeter in Space Radiation Fields

Firouz Payervand[1], GholamReza Raisali[1*], Fereshte Hajiesmaeilbaigi[2], Shahyar Saramad [3,4]

1. Radiation Applications Research School, Nuclear Science and Technology Research Institute, Atomic Energy Organization of Iran, Tehran, Iran
2. Laser and Optics Research School, Nuclear Science and Technology Research Institute, Atomic Energy Organization of Iran, Tehran, Iran
3. Faculty of Energy Engineering and Physics, Amirkabir University of Technology, Tehran, Iran
4. School of Particle and Accelerators, Institute for Research in Fundamental Sciences, Tehran, Iran

ARTICLE INFO

Article type:
Original Article

Article history:
Received: Jul 02, 2017
Accepted: Sep 13, 2017

Keywords:
Diamond Microdosimeter
Dose-Equivalent Response
Monte Carlo
Simulation

ABSTRACT

Introduction: Microdosimeters are helpful for dose equivalent measurement in unknown radiation fields. The favorable physical and mechanical properties of the detector-grade chemical vapor deposition diamond materials have made the diamond microdosimeters suitable candidate for radioprotection applications in space. The purpose of this work is the investigation of the dose equivalent response of a typical diamond microdosimeter with laser-induced graphitized electrodes for use in space radiation fields.

Materials and Methods: The Geant4 Monte Carlo simulation toolkit was applied to simulate the particle transport within the microdosimeter, and to determine the mean chord length and the dose equivalent response of the microdosimeter, based on the lineal energy dependent quality factor.

Results: The linear stopping power of the protons and alpha particles with energies higher than 5 MeV and 10 MeV respectively can be estimated within 20% of deviation using the microdosimeter response. The fluence to dose equivalent conversion coefficients calculated affirms that there is an adequate agreement between the calculated coefficients and other research group results.

Conclusion: The reasonable agreement between the dose equivalents calculated in this study and the results reported by other researchers confirmed that this type of microdosimeter could be a promising candidate suitable for the measurement of the dose equivalent in space radiation fields.

► *Please cite this article as:*
Payervand F, Raisali GH, Hajiesmaeilbaigi F, Saramad SH. Determination of Dose-Equivalent Response of A Typical Diamond Microdosimeter in Space Radiation Fields. Iran J Med Phys 2018; 15: 39-47. 10.22038/ijmp.2017.24503.1242.

Introduction

In the charged particle radiation fields comprising the protons in proton therapy and protons and alpha particles in space radiation fields, the radiation quality varies as the particles slow down and/or produce secondary particles. In such cases, the radiation field is unknown and made of several components. Therefore, it is practically impossible to determine the type and energy spectra of the radiation field for assessing the local linear energy transfer (LET)-dependent radiation quality with a simple and small device [1].

On the other hand, the radiation quality can be specified in terms of the stochastic lineal energy quantity, which is defined as the quotient of the energy imparted to matter in a volume of interest in a single event by the mean chord length of that volume [2, 3]. In 1950, Rossi et al. developed the first microdosimeter device, a low-pressure proportional counter, commonly called Rossi counter [4].

The standard measurement device in microdosimetry is a Rossi counter that is tissue equivalent [1, 5, 6]. Such microdosimeter is called the tissue equivalent proportional counter (TEPC). TEPC suffers from weaknesses such as low spatial resolution, requirement to high electrical power, and response dependency on pressure and temperature. However, semiconductor microdosimeters are good alternatives for overcoming these weaknesses.

Silicon microdosimeters were studied and compared with spherical TEPCs in 1980 by Dicello et al. [7]. They found significant differences between the microdosimetric spectra obtained by the two detectors. Nevertheless, they acknowledged the potential of silicon microdosimetry due to its high spatial resolution, in vivo capability, and pile-up robustness. Some disadvantages of these microdosimeters, such as the absence of tissue equivalency, low sensitivity, and low resistance to radiation, led to the development of more suitable microdosimeters. Diamond is considered to be very promising in this regard.

**Corresponding Author:* Radiation Applications Research School, Nuclear Science and Technology Research Institute, Atomic Energy Organization of Iran, Tehran, Iran, P.O. Box: 11365-3486, Tel: +9821-88221222, Fax: +9821-88221219, Email: graisali@aeoi.org.ir

Efforts to use diamond in radiation detection have begun since the early 1990s during which some reports highlighted the application of substances in dosimetry. For example, in 1997, Buttar et al. showed that the radiation sensitivity of diamond could be higher than silicon; as a result, such detectors were concluded to have superiority to silicon diodes and ion chambers [8]. The production of inexpensive chemical vapor deposition (CVD) diamonds with controlled and repeatable properties has been globally advanced in the recent years [9].

The microdosimeters that are based on the so-called detector-grade CVD diamond materials have been proposed for radiotherapy dosimetry and space radioprotection applications over the last few years. These microdosimeters have such favorable properties as more tissue equivalency, higher radiation hardness, lower temperature dependency, less dark current, as well as noise and sensitivity to visible light [10, 11].

The first attempt to obtain the spectra of energy deposition in an artificial diamond sensitive volume (SV) was presented by Angelone et al. [12]. They reported the comparison between simulations performed by the Monte Carlo method and the experimental tests performed with alphas to measure the dose distribution in terms of the lineal energy. They concluded that a high-purity monocrystalline CVD detector is suitable for the measurement of single-event depositions in micrometric sensitive volumes and collection of microdosimetric spectra of alpha radiation.

Rollet et al. discussed using of this microdosimeter as a new device to measure the dose distribution in terms of the lineal energy and the simulation performed by the Monte Carlo code FLUKA to optimize the design of the new one [11]. The characterization of a novel diamond microdosimeter prototype with 3D SVs produced by high energy boron implantation was established by Davis et al. [10]. They demonstrated that the proposed ion implantation technology allows for the formation of an array of well-defined 3D SVs. Furthermore, they developed a Geant4 application to explain the effect of aluminum electrode thickness on the observed anomaly in deposited energy. More details of the works of Davis can be observed in his thesis, which has been available recently [13].

Davis et al. created a diamond-based microdosimeter prototype featuring a 3D lateral electrode structure, using laser irradiation and active brazing alloys. They characterized it by means of ion beam induced charge collection measurements and finite element analysis [14]. The impact of the diamond detector geometry, in particular the elongated geometry of SV, the particles type (i.e., carbon ions or protons), and their energy, on the lineal energy distribution were studied by Solevi et al. through Monte Carlo simulations. They obtained important insights into the potentialities of CVD diamond detectors [15].

In order to use CVD diamond as a radiation detector, two electrodes are needed for applying the potential differences to collect the charge carriers by the positive and negative terminals. One of the methods for the creation of electrodes for diamond is making the graphitized electrodes by converting diamond to graphite as a conductive layer. Burgemeister [16] and Geis [17] were among the first pioneers who individually established a method to make a strong electrical contact in the regions with an increased conductivity created under laser irradiation.

Alemanno has recently used a similar method to create graphitized electrodes in a diamond detector [18]. He measured the electrical resistivity of the graphitized electrodes and demonstrated that this method facilitated the establishment of an ohmic contact. De Feudis et al. also characterized the integrated graphitic contacts on a diamond produced by means of laser irradiation [19]. One of the advantages of this method is that the electrodes are created in a single step at room temperature.

In another study, De Feudis et al. irradiated the surface of a detector grade CVD diamond sample by a laser beam to produce two sets of four parallel graphitic strip-like contacts along the whole sample both on the top and rear surfaces of the sample [20]. After an extensive characterization of the sample and investigation of the ohmic behavior of the diamond-graphite contact, they concluded that the laser writing technique was a good and fast solution to produce graphitic contacts on diamond surface, and therefore represented a promising way to fabricate segmented all-carbon devices.

The aim of this investigation is to determine the dose equivalent response of a typical diamond microdosimeter with electrodes produced by the laser-induced graphitization for the application in the space radiation fields. Therefore, considering the physical dimensions of the graphitized electrodes and also the created SV, the dose equivalent response of the microdosimeter is investigated using Geant4 Monte Carlo particle transport simulation toolkit.

The calculation methodology and the Geant4 application program developed in this study were verified by estimating the LET values of the monoenergetic protons and alpha particles and comparing them with the linear stopping powers reported by the National Institute of Standards and Technology (NIST) for water [21]. Moreover, the fluence to dose equivalent conversion coefficients for protons and alpha particles with some selected energies were calculated and the results were compared with the coefficients reported by Sato (2011) [22] and Roesler (2006) [23]. Finally, the verified application program was applied to calculate the microdosimeter dose equivalent response to galactic cosmic rays (GCRs) and solar particle events (SPEs).

Materials and Methods

In this section, the SV of the microdosimeter is described. Then, the role of the Monte Carlo tool in determining the microdosimeter response and simulating the particle transport within the microdosimeter is explained. Subsequently, the method of determining the mean chord length of the SV is presented. Since the microdosimeter intended in this study is considered to be applied in space radiation domain, the interplanetary radiation field is also specified.

Sensitive Volume Geometry of Microdosimeter

The irradiation of an undoped diamond substrate by a "Nd:YAG" laser beam would create graphitized electrodes with Gaussian cross-section as shown in Figure 1. The boundary regions of the SV of the detector are highlighted by applying 25 V electric potential to the central electrode and restricting the charge collection time to 50 ns (Figure 2). As can be seen, the geometry of the SV of microdosimeter was considered as 15 coaxial cylindrical slabs with different dimensions stacked on each other to form the whole volume.

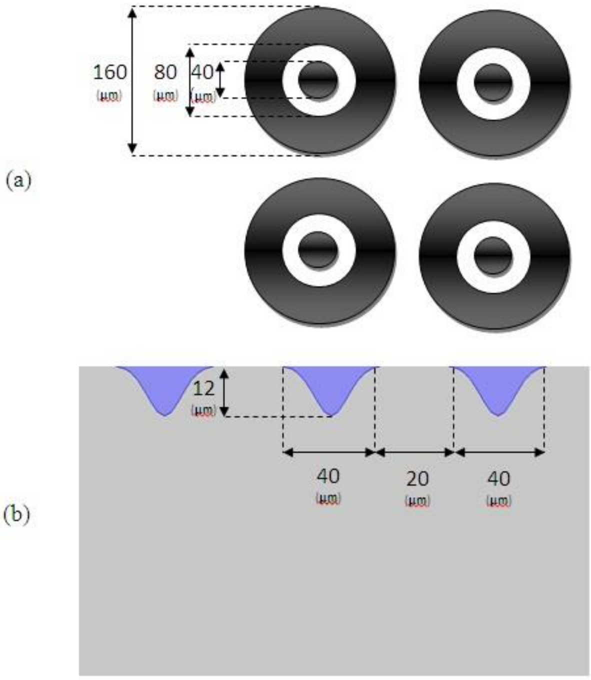

Figure 1. Schematic views of graphitized electrodes in diamond microdosimeter: a) top view, b) side view

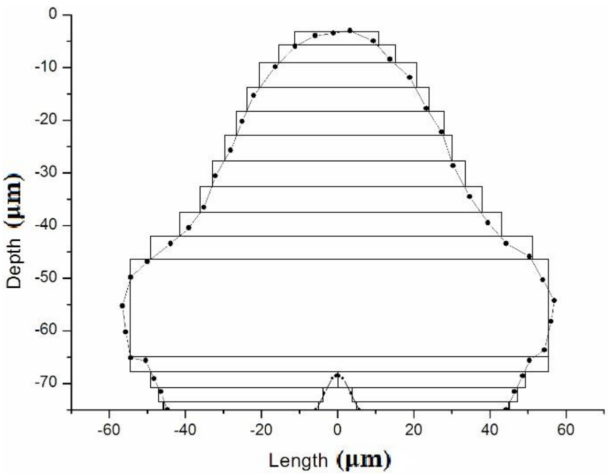

Figure 2. Layout and dimensions of sensitive volume in diamond microdosimeter formed by different coaxial slab cylinders stacked on each other

Monte Carlo Simulation

Geant4 toolkit with offering a comprehensive collection of physics processes over a wide range of energies, was used to simulate the passage of particles through matter and calculate the related energy depositions [24]. Geant4 has been used in a large number of experiments, projects, and a variety of applications [25]. Accordingly, the sufficiency of this toolkit for microdosimetric studies has been demonstrated in a number of previous research [5, 26, 27].

In this study, a Geant4 application was developed for modeling the electromagnetic and hadronic interactions of an incident proton or alpha particle in the SV of the diamond microdosimeter. Charge particles interact with the electrons and nuclei of the material through the electromagnetic force. Protons and alpha particles can also undergo a nuclear interaction. Charged particles with energies higher than 1 MeV, as is typical in nuclear phenomena, the energy is large, compared to the binding energy of the electrons in the atom.

To a first approximation, matter can be seen as a mixture of free electrons and nuclei at rest. The charged particle would feel the electromagnetic fields of the electrons and nuclei and undergo elastic collisions with these objects. In a collision with a nucleus, the charged particle would lose little energy; however, its direction can be changed completely. On the other hand, in collisions with electrons, a large amount of energy can be transferred to the electrons; nonetheless, the direction of the charged particle can only be slightly changed.

Secondary charged particles, which are produced in this way, have sufficient energy themselves to excite or ionize atoms in the medium. Other electromagnetic interactions of charged particles are multiple scattering or erratic changes in the direction of a particle along its trajectory, Cherenkov effect (or a light emission effect occurring whenever a charged particle travels in a medium faster than the speed of light in that medium), transition radiation (which is due to the polarization of the medium by the charged particle and depends on the plasma frequency in the material), and bremsstrahlung (or emission of electromagnetic radiation occurring when a charged particle undergoes acceleration or deviates from its trajectory due to a collision with a nucleus).

Moreover, at a high energy, all hadrons, on average, undergo a nuclear interaction after a distance approximately equal to the hadronic interaction length. In such a nuclear interaction, the target nucleus will be broken up. The nuclear fragments produced in this way are usually very unstable and return to a stable condition in several steps. One particular case that needs to be mentioned is the collision of a high-energy proton with a very heavy nucleus. A very heavy nucleus has many more neutrons than protons. If a very heavy nucleus is broken up in a collision with a high-energy proton, the fragments will quickly expel their excess neutrons; as a result, a large number of secondary neutrons are produced.

In Geant4 for the electromagnetic interactions, some physics processes were considered. These physics processes included pair production, photoelectric effect, Compton scattering, Rayleigh scattering, ionization, delta ray production, bremsstrahlung, and positron annihilation. Likewise, in the hadronic physics, two classes of processes, namely hadrons at rest (i.e., absorption, capture, and annihilation process) and hadrons in flight (i.e., elastic, inelastic, fission, and capture process) were taken into account.

Since QGSP-BIC-HP physics list of Geant4 toolkit has shown the best agreement with the experimental results in a proton radiation field [28], it was chosen for modeling the hadronic physics processes. Furthermore, in order to consider all electromagnetic interactions of the particles down to 250 eV, the Low Energy Physics Package based on Livermore data libraries [29] was selected in the development of our Geant4 application.

In the simulation, the incident particles were directed towards the SV within the vacuum. As schematically shown in Figure 3, a sphere with 1 m radius was considered around the SV as a source emitting the primary particles isotropically from a random point inwards with the cosine-law angular emission. In this way, since the generator surface is far enough from the SV, the distribution is practically isotropic [30]. In order to reduce the simulation time, the primary particle emission angle was limited to $0 \leq \theta < arctan\,(l/10^6)$, where l is the maximum length of the SV in μm.

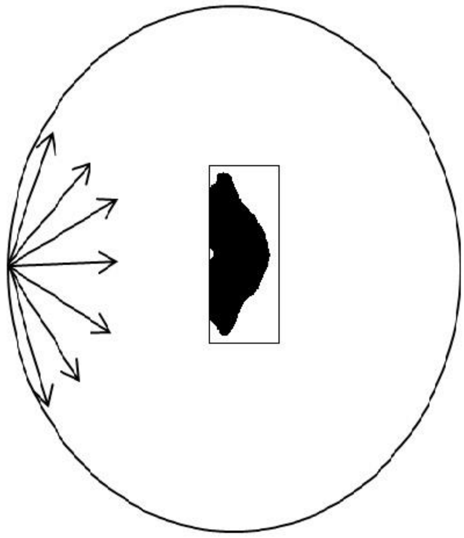

Figure 3. Schematic view of simulation setup showing a spherical surface source emitting primary particles isotropically from a random point inwards upon the sensitive volume located in the central part of the sphere

The primary and secondary particles were tracked in the simulation with a range cutoff of 0.01 μm. The output of the simulation was the energy deposition and track length per step in the SV. The number of incident particles for each case was selected large enough to achieve a relative statistical uncertainty less than 0.5% for the total energy deposition value in the SV.

Mean Chord Length Determination

The determination of the mean chord length of the SV is essential for specifying the lineal energy [2]. The mean chord length, "$\bar{l}$", of any convex shape can be calculated using Cauchy's theorem as given in equation 1:

$$\bar{l} = \frac{4V}{S} \qquad (1)$$

where, V is the volume, and S is the surface area of the sensitive volume. The mean chord length of the irregular geometric shapes can be calculated by their chord length, l, and distribution function, "$f(l)$", as follows [6]:

$$\bar{l}_F = \int_0^\infty l f(l) dl \qquad (2)$$

In this study, for various SV shapes, including the shape of the diamond microdosimeter, the chord length distribution function of the volume was calculated using the developed Geant4 application by defining Geantino as the incident radiation. Geantino is a virtual particle, which is used for simulation purposes and merely undertakes transportation processes without having any interaction with materials.

Interplanetary Radiation Field

From the radiation protection point of view, the most important components of the interplanetary space radiation environment include the GCRs and SPEs [31, 32]. The GCRs are composed of 87%, 12%, and 1% protons, helium ions, and heavier ions, respectively. The energy range of GCRs is within 10^6-10^{20} eV/nucleon. SPEs are also dominated by protons and alpha particles (90-95%). Heavy ions (Z>2) have a small contribution in SPEs. The energy range of SPEs is within from 10^5-10^{10} eV/nucleon.

Due to the importance and strength of GCR solar minimum occurred in 1977 (GCR-1977 solar minimum) [5], the differential fluxes for GCR protons and alpha particles in this solar minimum were used in this study. In addition, for the differential fluxes of SPE protons and alpha particles, we utilized the data corresponding to the "worst day model" averaged over 18 hours, begun on October 20, 1989 (SPE-Oct 1989) [5].

Microdosimeter Response Calculation

The absorbed dose, "D", is not sufficient to fully describe the biological effectiveness of the radiation. The dose equivalent quantity is defined for solving this problem. In this quantity, quality factor, Q, is used for considering the biological effectiveness of different types of radiations. The dose equivalent, H, is defined by the following equation (3):

$$H = D\bar{Q} \tag{3}$$

where $\bar{Q}$ is the effective quality factor of the radiation field.

In the ordinary dosimetry (macro-dosimetry), the effective quality factor is obtained by the following equation (4):

$$\bar{Q} = \int Q(L)d(L)dL \tag{4}$$

where, L is the linear energy transfer, and $Q(L)$ is the quality factor dependent on L. Moreover, $d(L)dL$ is the fraction of the absorbed dose due to the energy absorption of the charged particle with linear energy transfer in the range of L to L+dL. According to ICRP60, the quality factor depends on L as follows [33]:

$$Q(L) = \begin{cases} 1 & for \quad L < 10\ \frac{keV}{\mu m} \\ 0.32L - 2.2 & for \quad 10 \le L \le 100\ \frac{keV}{\mu m} \\ \frac{300}{\sqrt{L}} & for \quad L > 100\ \frac{keV}{\mu m} \end{cases} \tag{5}$$

In microdosimetry, the effective quality factor is obtained based on the quantity of the lineal energy, y:

$$\bar{Q} = \int Q(y)d(y)dy \tag{6}$$

where, $d(y)$ is the dose distribution of y for which $d(y)dy$ is the fraction of the absorbed dose due to the events in the range of y to y+dy. An event is a charged particle track, including a number of interactions within the SV. The $\bar{y}_F$ is the frequency-average of the lineal energy obtained by the following equation:

$$\bar{y}_F = \int yf(y)dy \tag{7}$$

To determine the lineal energy distribution for a given radiation and the SV size, the energy imparted to the SV in each ionization event was calculated and divided by the mean chord length of the SV. By setting the logarithmic bins of the lineal energy and scoring the frequency of events in each bin, the lineal energy distribution, "$f(y)$", was determined. After the determination of the lineal energy distributions, the dose equivalent response, H, was estimated by the equation (8) [34]:

$$H = D\int Q(y)\frac{yf(y)}{\bar{y}_F}dy \tag{8}$$

where $D = \frac{n\bar{l}_F\bar{y}_F}{m_{SV}}$ is the absorbed dose, $Q(y)$ is the quality factor, $\bar{l}_F$ is the mean chord length of the SV, m_{SV} is the mass of the SV, and n is the number of the events.

For a sphere site with 1 µm diameter, $Q(y)$ was obtained by the equation 9 [2]:

$$\mathrm{Q(y)} = 0.3y'\left[1 + \left(\frac{y'}{137}\right)^5\right]^{-0.4} \tag{9}$$

where, y' is given by equation 10 [35]:

$$y' = \frac{9}{8}y + \frac{\delta_2}{\bar{l}} \tag{10}$$

where, y is the measured lineal energy in keV/µm, $\bar{l}$ is the mean chord length of the sphere in µm, and δ_2 is the weighted average of the energy imparted to the site by the individual delta rays in keV.

In this study, the frequency-averaged lineal energy of the monoenergetic protons and alpha particles was calculated by equation 7. Then, assuming that $L = \bar{y}_F$, the linear energy transfer was estimated. Since the linear stopping power was equal to the linear energy transfer, this quantity was compared with the linear stopping power of water reported by the NIST [21]. In addition, the dose equivalent response of the microdosimeter was obtained for monoenergetic protons in the range of 10 MeV to 100 GeV by equation 8.

The fluence to dose equivalent conversion coefficients were also calculated in $\frac{pSv}{cm^2}$ and compared with those reported by Sato [22] and Roesler [23]. Finally, for the investigation of the dose equivalent response of the microdosimeter in the space radiation fields, the definitions of the quantities were extracted from the International Atomic Energy Agency Safety Standards Series No. GSR Part 3 (2014) [36]. Subsequently, the interplanetary radiation environment was combined with Geant4 toolkit, and the microdosimeter dose equivalent response was obtained for GCR and SPEs.

Results

Mean Chord Length Study

In this part of the study, the results of the chord lengths study of the regular geometries as well as the SV of the microdosimeter are provided. The chord length distribution function of the SV of the microdosimeter is illustrated in Figure 4. Calculations based on this function by applying equation 2 indicated that the mean chord length of the diamond microdosimeter under study was 49 µm, which was larger than the ideal of about 1 µm.

Table 1 presents the mean chord length calculated by the equations given in Section 2.3. The results demonstrated that the differences of the applied method with the Cauchy's theorem were less than 2% for regular geometries. Due to the complex geometry of the SV of the diamond microdosimeter, its chord length was calculated by the Monte Carlo simulation using Geantino null particle.

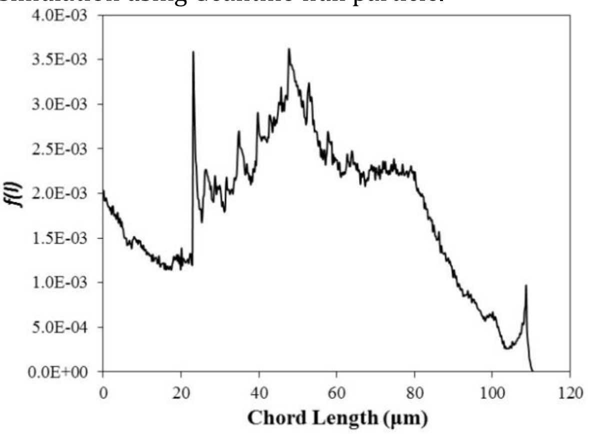

Figure 4. Chord length distribution function of diamond microdosimeter

Investigation of Linear Energy Transfer by Microdosimeter Response

Figure 5 shows the ratio of the frequency-averaged lineal energy of monoenergetic protons and alpha particles determined by the microdosimeter response to the linear stopping power reported by NIST for water [21]. The linear stopping power of the protons with energies greater than 5 MeV can be estimated using the studied microdosimeter with a relative error less than 20%. Nonetheless, for alpha particles, this relative error criterion occurs in energies greater than 10 MeV. Moreover, the figure shows that the ratio of the frequency-averaged lineal energy decreases severely in the energies less than 5 MeV and 10 for protons and alpha particles, respectively.

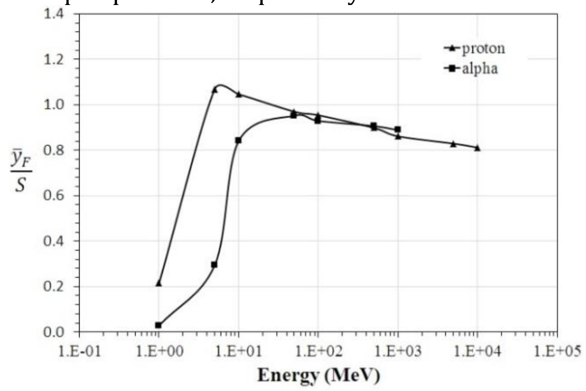

Figure 5. Ratio of calculated frequency-averaged lineal energy, "$\bar{y}_F$", of diamond microdosimeter to linear stopping power, "S", for various proton and alpha particle energies (the linear stopping powers for water are taken from NIST [21])

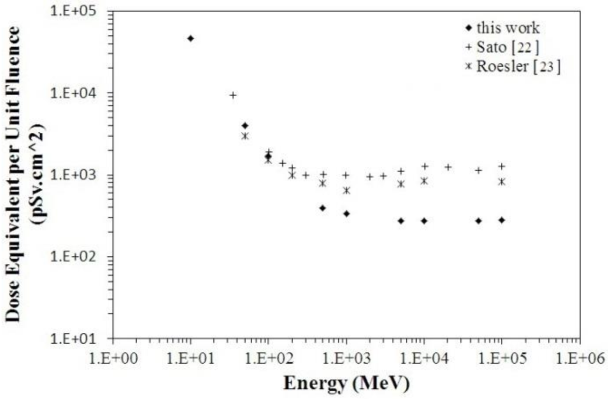

Figure 6. Fluence to dose equivalent conversion coefficients of monoenergetic protons estimated by diamond microdosimeter by applying Q (y) using equation 9 and those reported by Sato [22] and Roesler [23]

Microdosimeter Response to Monoenergetic Proton and Alpha Particles and for Space Radiation Fields

Sato [22] and Roesler [23] individually calculated the fluence to ambient dose equivalent conversion coefficients, $H^*(10)$, by PHITS and FLUKA codes, respectively, based on the quality factor recommended by ICRP60 [33]. Figure 6 illustrates the fluence to dose equivalent conversion coefficients for monoenergetic protons in the range of 10 MeV to 100 GeV, determined by the microdosimeter by applying *Q(y)* and those reported by Sato and Roesler [22, 23].

According to Figure 6, there was an acceptable agreement between the coefficients estimated in the present study and those obtained by the above mentioned researchers. However, for energies greater than 100 MeV, our calculations were inconsistent with those reported by Sato and Roesler [22, 23]. This discrepancy was due to the differences in the quality factors. The fluence to dose equivalent conversion coefficients for the monoenergetic protons estimated by the microdosimeter by applying *Q(L)* and those reported by Sato and Roesler [22, 23] are also shown in Figure 7. As can be seen, by applying *Q(L)* instead of *Q(y)* in our calculation, the difference is ignorable.

Figure 8 shows the lineal energy distribution obtained by the microdosimeter for GCR-1977 solar minimum and SPE-Oct 1989 spectrums. The dose equivalents calculated by GCR-1977 solar minimum and the SPE-Oct 1989 spectrums were 61.2 cSv/year and 2.82×10^3 cSv/event, respectively. These calculations were in reasonable agreement with the dose equivalent of free space reported previously as 62.1 cSv/year and 2.5×10^3 cSv/event, respectively [37-40].

Table 1. Comparison of mean chord length calculated by equations 2 and 1

	Sphere	Hemisphere	Spheroid	Cylinder	Cube	Rectangular parallelpiped
Calculated (µm)	13.33±0.13	8.89±0.09	7.44±0.07	13.33±0.13	13.33±0.13	11.43±0.11
Monte Carlo estimated (µm)	13.33±0.14	8.87±0.9	7.31±0.07	13.35±0.14	13.33±0.14	11.41±0.11
Relative error (%)	0.02	0.26	1.720	0.16	0.01	0.16

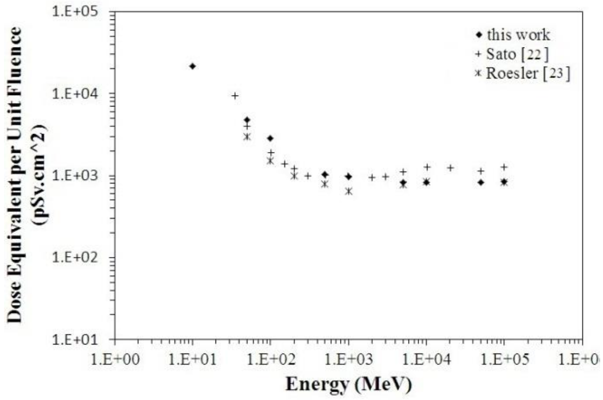

Figure 7. Fluence to dose equivalent conversion coefficients for monoenergetic protons estimated by diamond microdosimeter by applying Q (L) using equation 5 and those reported by Sato [22] and Roesler [23]

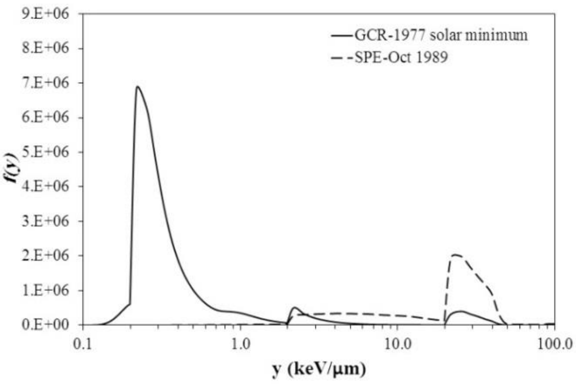

Figure 8. Calculated lineal energy distribution in diamond microdosimeter for GCR-1977 solar minimum and SPE-Oct 1989

Discussion

According to the data presented in Table 1, the differences of the applied method with the Cauchy's theorem were less than 2%. This means that we can rely on the calculation of the mean chord length of SVs by the method presented in Section 2.3 using the developed application program.

The severe decrease in the ratio of the frequency-averaged lineal energy in the energies less than 5 MeV for protons and less than 10 MeV for alpha particles, shown in Figure 5, could be related to the dimensions of the microdosimeter SV.

Since, most of the protons and alpha particles with these energies were stopped within such SVs without crossing the boundaries, the amount of their lineal energies, and consequently the frequency-averaged lineal energies underestimated the linear stopping power. The linear stopping power of the protons and alpha particles with energies greater than 5 and 10 MeV, respectively, were estimated with a relative error of less than 20%. The absorbed dose and dose equivalent were expected to be determined within an acceptable uncertainty for radiation protection applications.

The lack of full compliance between the fluence to dose equivalent conversion coefficients estimated in this study and those reported in other studies (Figure 6) is due to the difference between the LET-based and lineal energy-based quality factors. The formers are recommended by ICRP60 in equation 5 and the latters are provided in equation 9. By increasing the proton energy, LET decreases to less than 10 $keV/\mu m$ from which the quality factor applied here as $Q(y)$ was several times less than $Q(L)$ used by other investigators.

Based on Figure 7, the utilization of $Q(L)$ instead of $Q(y)$ would facilitate a satisfactory agreement between the coefficients. Based on the reasonable consistency between the coefficients estimated in the present study and those obtained by others, the studied diamond microdosimeter was predicted to be able to measure the dose equivalent of the protons with energies more than 10 MeV with an acceptable accuracy.

Conclusion

The microdosimeter response study indicated that the linear stopping power of the protons and alpha particles with energies greater than 5 and 10 MeV, respectively, could be estimated with a relative error less than 20%. The investigation of the fluence to dose equivalent conversion coefficients of the monoenergetic protons indicated an adequate agreement between the coefficients calculated by the microdosimeter in the present study and those obtained by other investigators.

Therefore, the studied microdosimeter was predicted to be able to measure the dose equivalent of the protons with energies higher than 10 MeV, which is of interest in space applications. The reasonable agreement between the dose equivalent calculated based on the GCR-1977 solar minimum spectrum and the SPE-Oct 1989 spectrum in this study and the results reported by other researchers confirmed that this type of microdosimeter could be a promising candidate suitable for the measurement of the dose equivalent in space radiation fields regarding other favorable properties of diamond, including more tissue equivalency and higher radiation hardness.

Acknowledgement

This study has received substantial support from the Nuclear Science and Technology Research Institute of Atomic Energy organization of Iran.

References

1. Verona C, Magrin G, Solevi P, Grilj V, Jakšić M, Mayer R, et al. Spectroscopic properties and radiation damage investigation of a diamond based Schottky diode for ion-beam therapy microdosimetry. Journal of Applied Physics. 2015;118(18):184503.
2. The quality factor in radiation protection: report of a joint task group of the ICRP and the ICRU to the ICRP and the ICRU. International Commission on Radiation Units and Measurements; 1986. Contract No.: 40.
3. Rossi BHH, Zaider M. Microdosimetry and its Applications: Springer; 1996.
4. Rossi HH, Rosenzweig W. A device for the measurement of dose as a function of specific ionization. Radiology. 1955;64(3):404-11.
5. Davis JA, Guatelli S, Petasecca M, Lerch ML, Reinhard MI, Zaider M, et al. Tissue equivalence study of a novel diamond-based microdosimeter for galactic cosmic rays and solar particle events. IEEE Transactions on Nuclear Science. 2014;61(4):1544-51.
6. Bradley PD. The development of a novel silicon microdosimeter for high LET radiation therapy: University of Wollongong; 2000.
7. Dicello J, Amols H, Zaider M, Tripard G. A comparison of microdosimetric measurements with spherical proportional counters and solid-state detectors. Radiation Research. 1980;82(3):441-53.
8. Buttar C, Conway J, Meyfarth R, Scarsbrook G, Sellin P, Whitehead A. CVD diamond detectors as dosimeters for radiotherapy. Nuclear Instruments and Methods in Physics Research Section A: Accelerators, Spectrometers, Detectors and Associated Equipment. 1997;392(1-3):281-4.
9. De Angelis C, Bucciolini M, Casati M, Løvik I, Bruzzi M, Lagomarsino S, et al. Improvements in CVD diamond properties for radiotherapy dosimetry. Radiation protection dosimetry. 2006;120(1-4):38-42.
10. Davis JA, Ganesan K, Alves AD, Guatelli S, Petasecca M, Livingstone J, et al. Characterization of a novel diamond-based microdosimeter prototype for radioprotection applications in space environments. IEEE Transactions on Nuclear Science. 2012;59(6):3110-6.
11. Rollet S, Angelone M, Magrin G, Marinelli M, Milani E, Pillon M, et al. A novel microdosimeter based upon artificial single crystal diamond. IEEE Transactions on Nuclear Science. 2012;59(5):2409-15.
12. Angelone M, Magrin G, Pillon M, Prestopino G, Rollet S, Milani E, et al. Simulation and test of a new MicroDosimeter based upon Single Crystal Diamond. Nuclear Science Symposium and Medical Imaging Conference (NSS/MIC), 2011 IEEE: IEEE; 2011. p. 1738-41.
13. Davis JA. Diamond microdosimetry for radioprotection applications in space: University of Wollongong; 2015.
14. Davis JA, Ganesan K, Prokopovich DA, Petasecca M, Lerch ML, Jamieson DN, et al. A 3D lateral electrode structure for diamond based microdosimetry. Applied Physics Letters. 2017;110(1):013503.
15. Solevi P, Magrin G, Moro D, Mayer R. Monte Carlo study of microdosimetric diamond detectors. Physics in medicine and biology. 2015;60(18):7069.
16. Burgemeister EA, inventor; U.S. Patent No. 4,511,783, assignee. Method for making electrical contacts to diamond by means of a laser, and diamond provided with contacts according to this optical method patent 4511783. 1985.
17. Geis MW, Rothschild M, Ehrlich DJ, inventors; U.S. Patent No. 5,002,899, assignee. Electrical contacts on diamond patent 5002899. 1991.
18. E. Alemanno AC, M. Catalano, G. Chiodini, G. Fiore, M. Martino, R. Perrino, C. Pinto, S. Spagnolo. Diamond detector with laser made graphitic electrodes. Italy: Istituto Nazionale di Fisica Nucleare; 2011.
19. De Feudis M, Caricato A, Martino M, Alemanno E, Ossi P, Maruccio G, et al. Realization and characterization of graphitic contacts on diamond by means of laser. 4th Workshop-Plasmi, Sorgenti, Biofisica ed Applicazioni; 2015: 63-8.
20. De Feudis M, Caricato A, Taurino A, Ossi P, Castiglioni C, Brambilla L, et al. Diamond graphitization by laser-writing for all-carbon detector applications. Diamond and Related Materials. 2017;75:25-33.
21. Berger MJ, Coursey J, Zucker M, Chang J. Stopping-power and range tables for electrons, protons, and helium ions: NIST Physics Laboratory; 1998.
22. Sato T, Endo A, Zankl M, Petoussi-Henss N, Yasuda H, Niita K. Fluence-to-dose conversion coefficients for aircrew dosimetry based on the new ICRP Recommendations. Progress in Nuclear Science and Technology. 2011;1:134-7.
23. Stefan Roesler GRS. A FLUKA user-routine converting fluence into effective dose and ambient dose equivalent. Switzerland: EUROPEAN ORGANIZATION FOR NUCLEAR RESEARCH, CERN; 2006.
24. Agostinelli S, Allison J, Amako Ka, Apostolakis J, Araujo H, Arce P, et al. GEANT4—a simulation toolkit. Nuclear instruments and methods in physics research section A: Accelerators, Spectrometers, Detectors and Associated Equipment. 2003;506(3):250-303.
25. Allison J, Amako K, Apostolakis Jea, Araujo H, Dubois PA, Asai M, et al. Geant4 developments and applications. IEEE Transactions on Nuclear Science. 2006;53(1):270-8.
26. Guatelli S, Reinhard MI, Mascialino B, Prokopovich DA, Dzurak AS, Zaider M, et al. Tissue equivalence correction in silicon microdosimetry for protons characteristic of the LEO space environment. IEEE Transactions on Nuclear Science. 2008;55(6):3407-13.

27. Anjomani Z, Hanu A, Prestwich W, Byun S. Monte Carlo design study for thick gas electron multiplier-based multi-element microdosimetric detector. Nuclear Instruments and Methods in Physics Research Section A: Accelerators, Spectrometers, Detectors and Associated Equipment. 2014;757:67-74.
28. Jarlskog CZ, Paganetti H. Physics settings for using the Geant4 toolkit in proton therapy. IEEE Transactions on Nuclear Science. 2008;55(3):1018-25.
29. Chauvie S, Guatelli S, Ivanchenko V, Longo F, Mantero A, Mascialino B, et al. Geant4 low energy electromagnetic physics. Nuclear Science Symposium Conference Record, 2004 IEEE: IEEE; 2004: 1881-5.
30. Santin G. Normalisation modelling sources. Geant4Tutorial; Paris, France: 2007.
31. Dietze G, Bartlett D, Cool D, Cucinotta F, Jia X, McAulay I, et al. ICRP Publication 123: Assessment of Radiation Exposure of Astronauts in Space. ICRP Publication 123. 2013;42(4):1-339.
32. Spurný F. Space and Flights Radiation Protection. Czech Academy of Sciences, Prague, Czech Republic: Nuclear Physics Institute; 2008.
33. 1990 Recommendations of the International Commission on Radiological Protection. ICRP Publication 60. 1991;21(1-3).
34. Prokopovich DA. Silicon on insulator microdosimetry for radiation protection in mixed radiation fields for aviation and space dosimetry: University of Wollongong; 2010.
35. Kellerer AM, Hahn K. Considerations on a revision of the quality factor. Radiation research. 1988;114(3):480-8.
36. Agency IAE. Radiation Protection and Safety of Radiation Sources: International Basic Safety Standards: International Atomic Energy Agency; 2014.
37. Lin Z-W. Can the Equivalent Sphere Model Approximate Organ Doses in Space? 18th Annual NASA Space Radiation Investigator's Workshop; Rohnert Park, CA; United States2007.
38. Clowdsley MS, Wilson JW, Kim M-H, Anderson BM, Nealy JE. Radiation protection quantities for near Earth environments. 2004.
39. Borggräfe A, Quatmann M, Nölke D. Radiation protective structures on the base of a case study for a manned Mars mission. Acta Astronautica. 2009;65(9):1292-305.
40. Hu S, Kim M-HY, McClellan GE, Cucinotta FA. Modeling the acute health effects of astronauts from exposure to large solar particle events. Health physics. 2009;96(4):465-76.